The Conformational Potential Energy Surface of Glycine: A Theoretical Study

Jan H. Jensen and Mark S. Gordon*

Contribution from the Department of Chemistry, North Dakota State University, Fargo, North Dakota 58105. *Received March 7, 1991*

Abstract: The conformational potential energy surface of nonionized glycine has been studied by using ab initio (6-31G*, STO-2G) and semiempirical (AM1, PM3) methods. The MP2/6-31G*//RHF/6-31G* potential energy surface was then used to calculate the Boltzmann equilibrium distribution and kinetics of conformational interconversion at various temperatures. The results of this study are compared to previous computational and experimental investigations of gas-phase glycine.

Introduction

Isolated amino acids exist in the gas phase in the nonionized form $NH_2CHRCOOH$, where R = H for glycine—the simplest of the roughly 21 amino acids common in nature. Glycine is simply an amino group and a carboxyl group separated by a saturated carbon. This structure has three internal rotational degrees of freedom: the rotation of the hydroxyl group around the C–O bond, the rotation around the C–C bond, and the rotation of the amino group around the C–N bond.

The objective of this paper is to present a theoretical study of the conformational potential energy surface (PES) of the α-amino carboxylic acid glycine in the nonionized form. An important part of this study is to make a thorough comparison between ab initio and semiempirical (AM1 and PM3) Hamiltonians with regard to structure, relative energies, normal modes, and characterizations of stationary points. A subset of the possible minima on the glycine PES is summarized in Scheme I.

The use of ab initio methods to study this problem began when Vishveshwara and Pople[1] published RHF/4-31G energies of several conformations (with standard bond lengths and angles) assumed to be stationary points. They predicted the torsional parameters for their global minimum conformation (GLY1 in Scheme I) but were unable to verify this structure with computation or experiment. The latter was rectified when two microwave studies of gas-phase glycine were published independently.[2,3] Neither group found the global minimum predicted by Vishveshwara and Pople. Instead the experimental structure corresponded to a conformer (GLY3) that was 2.2 kcal/mol above the theoretical minimum.[1] This apparent disagreement between theory and experiment was investigated by Sellers and Schäfer[4] who fully optimized the structure of both conformations at the RHF/4-21G level and found that (1) the energy difference remained 2.2 kcal/mol (GLY1 lower) and (2) the conformer observed experimentally had a much larger calculated dipole moment (6.54 vs 1.10 D). The latter, they argued, made the second conformer more visible in the microwave spectrum. Later, using a more sensitive instrument, a microwave structure (GLY1) was observed by Suenram and Lovas[5] and verified as the global minimum by Schäfer et al.[6] who optimized a third conformer (GLY2) at the RHF/4-21G level to provide additional evidence.

Palla et al.[7] mapped PESs for glycine in the nonionized and zwitterionic states with four different methods: RHF/STO-3G,[8] CNDO,[9] PCILO,[10] and a classical potential. They found significant differences in the surface predicted by STO-3G and the surface predicted by Vishveshwara and Pople, although GLY1 remained the global minimum. All other methods failed to even locate this experimental global minimum.

In 1984, Luke et al.[11] reported RHF/STO-3G optimized structures for the eight possible C_s conformations of glycine and compared these, when possible, to the relative energies of Vishveshwara and Pople's study. No force fields were calculated to determine the nature of these stationary points. Masamura used the three 4-21G optimized structures of Schäfer et al.[6] plus optimized structures of other amino acids to assess the reliability of MNDO[12] and AM1[13] and found that both performed satisfactorily, although AM1 performed better than MNDO.

Very recently, Ramek[14] published a vibrational analysis of GLY3 at the 4-31G level of theory. He showed that GLY3 is

Scheme I. Possible C_s Stationary Points on the Conformational PES of Glycine

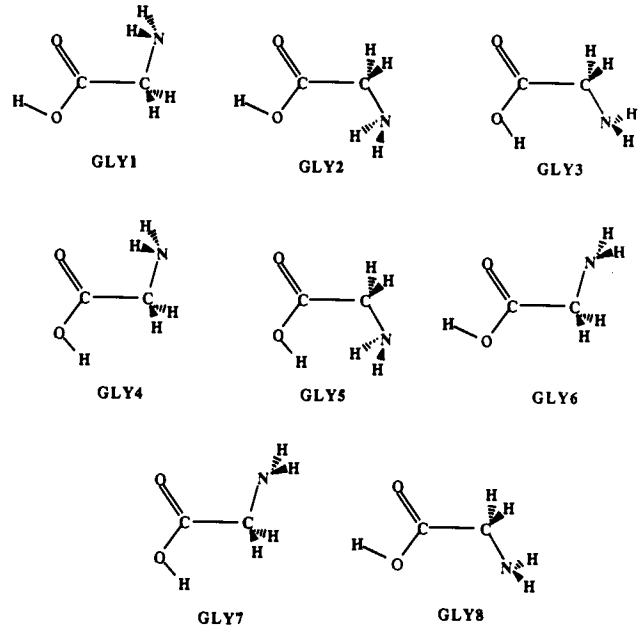

(1) Vishveshwara, S.; Pople, J. A. *J. Am. Chem. Soc.* **1977**, *99*, 2422.
(2) Brown, R. D.; Godfrey, P. D.; Storey, J. W. V.; Bassez, M. P. *J. Chem. Soc., Chem. Commun.* **1978**, 547.
(3) Suenram, R. D.; Lovas, F. J. *J. Mol. Spectrosc.* **1978**, *72*, 372.
(4) Sellers, H. L.; Schäfer, L. *J. Am. Chem. Soc.* **1978**, *100*, 7728.
(5) Suenram, R. D.; Lovas, F. J. *J. Am. Chem. Soc.* **1980**, *102*, 7180.
(6) Schäfer, L.; Sellers, H. L.; Lovas, F. J.; Suenram, R. D. *J. Am. Chem. Soc.* **1980**, *102*, 6566.
(7) Palla, P.; Petrongolo, C.; Tomasi, J. *J. Phys. Chem.* **1980**, *84*, 435.
(8) (a) Hehre, W. J.; Stewart, R. F.; Pople, J. A. *J. Chem. Phys.* **1969**, *51*, 2657. (b) Hehre, W. J.; Ditchfield, R.; Stewart, R. F.; Pople, J. A. *J. Chem. Phys.* **1970**, *52*, 2769. (c) Gordon, M. S.; Bjorke, M. D.; Marsh, F. J.; Korth, M. S. *J. Am. Chem. Soc.* **1978**, *100*, 2670.
(9) (a) Pople, J. A.; Santry, D. P.; Segal, G. A. *J. Chem. Phys.* **1965**, *43*, 129. (b) Pople, J. A.; Segal, G. A. *J. Chem. Phys.* **1965**, *43*, 136. (c) *Ibid.* **1966**, *44*, 3289. (d) Pople, J. A.; Beveridge, D. L. *Approximate Molecular Orbital Theory*; McGraw-Hill: New York, 1970.
(10) (a) Diner, S.; Malrieu J. P.; Claverie, P. *Theor. Chim. Acta* **1969**, *13*, 1. (b) Malrieu, J. P.; Claverie, P.; Diner, S. *Ibid.* **1969**, *13*, 18. (c) Diner, S.; Malrieu, J. P.; Jordan, F.; Giblert, *Ibid.* **1969**, *15*, 100.
(11) Luke, B. T.; Gupta, A. G.; Loew, G. H.; Lawless, J. G.; White, D. H. *Int. J. Quantum Chem., Quantum Biol. Symp.* **1984**, *11*, 117.
(12) Masamura, M. *J. Mol. Struct.* **1987**, *152*, 293.
(13) Masamura, M. *J. Mol. Struct.* **1988**, *164*, 299.
(14) Ramek, M. *Int. J. Quantum Chem., Quantum Biol. Symp.* **1990**, *17*, 45.

0002-7863/91/1513-7917$02.50/0

Table I. Relative Energies (kcal/mol) of the Eight C_s Conformers[a]

basis set	GLY1	GLY2	GLY3	GLY6	GLY8	GLY4	GLY5	GLY7
MP2/6-31G*//RHF/6-31G*	0.0	1.7	1.8	5.8	6.5	6.5	8.4	13.3
RHF/6-31G*//RHF/6-31G*	0.0^{M}	1.9^{M}	3.2^{T}	5.6^{T}	6.1^{B}	7.0^{M}	9.3^{M}	13.6^{T}
RHF/6-31G*//RHF/STO-2G	0.0	2.3	3.9	6.1	7.5	7.9	11.6	15.4
RHF/6-31G*//PM3	0.0	2.1	7.5	6.2	13.1	9.2	13.4	16.5
RHF/6-31G*//AM1	0.0	2.2	6.2	7.5	6.7	7.6	11.4	14.3
RHF/STO-2G//RHF/STO-2G	0.0^{M}	0.6^{T}	2.0^{T}	4.8^{T}	5.8^{B}	4.1^{M}	7.7^{T}	9.8^{T}
PM3//PM3	0.0^{M}	1.1^{M}	4.2^{T}	4.6^{B}	5.2^{B}	3.6^{M}	6.8^{T}	7.7^{B}
AM1//AM1	0.0^{M}	0.4^{M}	8.2^{T}	6.2^{B}	6.9^{B}	6.0^{M}	9.1^{T}	12.6^{T}

[a] The nature of each stationary point is indicated as a superscript by M (minimum), T (transition state), and B (barrier).

a minimum on the RHF/4-31G PES.

In summary, three C_s conformers (GLY1–3) have been optimized with RHF/4-21G and all eight C_s conformers have been optimized with RHF/STO-3G. The torsional parameters and relative energies for some assumed conformational transition states were reported.[1] Only one force field to confirm the nature of these stationary points has been published.

Computational Methods

For the ab initio calculations, two basis sets were employed. Molecular structures were determined at the restricted Hartree–Fock (RHF) level, using the 6–31G*[15] and the STO–2G[16] basis sets. All stationary points were verified to be either minima or transition states on the PES by establishing that their matrices of second derivatives (hessians) were positive definite or had one, and only one, negative eigenvalue upon diagonalization, respectively. The hessians were all determined analytically. As part of the extensive probing of the glycine PES, several linear least motion paths (LLMP) were investigated. The hessians for the highest energy conformers on these paths were calculated with the 3-21G[17] basis set to economize computer time.

Single-point energies using second-order Møller–Plesset perturbation theory (MP2[18]) with the 6-31G* basis set were performed on RHF/6-31G* structures (this is denoted MP2/6-31G*//RHF/6-31G*). Single-point RHF/6-31G* energies were performed on structures obtained with STO-2G, AM1,[19] and PM3.[20] All ab initio calculations were performed with either GAUSSIAN86[21] or GAMESS.[22]

The semiempirical calculations were performed with the MOPAC network of programs (version 5.0),[23] using the AM1 and the newly developed PM3 Hamiltonians. All transition states were characterized as described above, but the hessians were computed numerically. The C_s transition states were, whenever possible, identified by following the gradient downhill in both directions by using the gradient-following algorithm implemented in MOPAC.

A method was devised to gauge the similarity of two transition states, obtained with different computational methods, by comparing the eigenvectors associated with the negative eigenvalues. This direct mode comparison (DMC) calculates the mass-weighted dot product of the two normalized eigenvectors and judges their similarity by how little the dot product (DMC index) deviates from unity. Similar eigenvectors indicate that the transition states are similar, if not identical, and also suggests that the results obtained by following the minimum energy path (MEP) from the transition state obtained at one level of theory will apply to the transition state obtained at the higher level of theory.

The Gibbs free energy was calculated by using standard statistic-mechanical formulae[24] (with the harmonic oscillator–rigid rotor approximation) as implemented in GAMESS. All real frequencies were scaled by 0.89 before they were used in these calculations.

The vibrational decomposition scheme used to decompose frequencies is that implemented in GAMESS.[25]

Table II. Average Deviations (6-31G* – X) of Bond Lengths, Bond Angles, and Dihedrals for X = STO-2G, PM3, and AM1[a]

param	STO-2G	PM3	AM1
	Bond Lengths		
r(CC)	−0.053 ± 0.004	0.003 ± 0.002	0.005 ± 0.003
r(C=O)	−0.034 ± 0.003	−0.031 ± 0.001	0.047 ± 0.001
r(C—O)	−0.064 ± 0.004	−0.023 ± 0.004	−0.034 ± 0.004
r(OH)	−0.046 ± 0.002	0.001 ± 0.002	−0.018 ± 0.003
r(CN)	−0.048 ± 0.007	−0.031 ± 0.004	0.011 ± 0.004
r(CH)	−0.013 ± 0.002	−0.024 ± 0.002	−0.043 ± 0.003
r(NH)	−0.042 ± 0.001	0.002 ± 0.001	0.002 ± 0.002
	Bond Angles		
A(CC=O)	−0.7 ± 1.5	−4.0 ± 0.3	−3.3 ± 0.9
A(CC—O)	0.5 ± 2.0	−5.2 ± 2.0	−3.6 ± 1.9
A(HOC)	4.9 ± 1.3	−1.0 ± 1.5	−0.6 ± 1.8
A(NCC)	1.9 ± 1.5	1.4 ± 1.1	−0.5 ± 0.7
A(HCC)	−1.6 ± 0.5	−1.6 ± 0.3	0.5 ± 0.2
A(HNC)	5.2 ± 1.1	1.9 ± 1.5	−0.2 ± 1.2
	Dihedral Angles		
D(O=CCH)	−0.9 ± 0.3	−1.0 ± 0.2	−0.8 ± 0.2
D(CCNH)	0.0 ± 6.7	−0.4 ± 2.4	1.0 ± 2.5

[a] Bond length, Å; bond and dihedral angles, deg.

Results and Discussion

A. C_s Conformers. The eight conformers of nonionized glycine, presented in Scheme I, were optimized within the C_s point group at the RHF/6-31G*, RHF/STO-2G, PM3, and AM1 levels of theory, and characterized by calculating the hessians. The usefulness of RHF/STO-2G, PM3, and AM1 in the study of glycine can be gauged by comparison to 6-31G* for the following properties: (1) relative energy, (2) geometry, (3) number of imaginary frequencies.

The relative energies, calculated with various basis sets, are listed in Table I. The effect of correlation (MP2 energy correction) does not appear to be significant: The relative energy changes most for GLY3 and then only by 1.4 kcal/mol. Therefore, the remaining calculations were performed at the SCF level of theory. The order, in terms of stability, predicted by the highest level of theory is duplicated by RHF/6-31G*//RHF/6-31G* and by RHF/6-31G*//RHF/STO-2G.

The predicted energy range from GLY1 to GLY8 is smaller for STO-2G and PM3. Both RHF/STO-2G and PM3 reproduce the trends reasonably well, but underestimate the relative energy of GLY4 by 2–3 kcal/mol and of GLY7 by 4–6 kcal/mol. AM1 overestimates the relative energy of GLY3 by 6.4 kcal/mol. This, apparently, is due to the inability of AM1 to account for intramolecular hydrogen bonding. The 6-31G* basis set predicts an OH···N distance of 2.02 Å, well within hydrogen-bonding range, whereas AM1 predicts 2.34 Å. This is reflected in the structure

(15) Hariharan, P. C.; Pople J. A. *Theor. Chim. Acta* **1973**, *28*, 213.
(16) (a) Hehre, W. J.; Stewart, R. F.; Pople J. A. *J. Chem. Phys.* **1969**, *51*, 2657. (b) Hehre, W. J.; Ditchfield, R.; Stewart, R. F.; Pople, J. A. *J. Chem. Phys.* **1970**, *52*, 2769. (c) Gordon, M. S.; Bjorke, M. D.; Marsh, F. J.; Pople, J. A. *J. Am. Chem. Soc.* **1978**, *100*, 2670.
(17) Binkley, J. S.; Pople, J. A.; Hehre, W. J. *J. Am. Chem. Soc.* **1980**, *102*, 939.
(18) Krishnan, R.; Pople, J. A. *Int. J. Quantum Chem.* **1978**, *14*, 91.
(19) Dewar, M. J.; Zoebisch, E. G.; Healy, E. F.; Stewart, J. J. P. *J. Am. Chem. Soc.* **1985**, *107*, 3902.
(20) (a) Stewart, J. J. P. *J. Comput. Chem.* **1989**, *10*, 209. (b) *Ibid.* **1989**, *10*, 221.
(21) Frisch, M. J.; Binkley, J. S.; Schlegel, H. B.; Raghavashari, K.; Melius, C. F.; Martin, R. L.; Stewart, J. J. P.; Brobrowicz, F. W.; Rohlfing, C. M.; Kahn, L. R.; DeFrees, D. J.; Seeger, R.; Whiteside, R. A.; Fox, D. J.; Fluder, E. M.; Topiol, S.; Pople, J. A. GAUSSIAN86; Carnegie Mellon Quantum Chemistry Publishing Unit: Pittsburgh, PA 15213.
(22) Schmidt, M. W.; Baldridge, K. K.; Boatz, J. A.; Jensen, J. H.; Koseki, S.; Gordon, M. S.; Nguyen, K. A.; Windus, T. L.; Elbert, S. T. *QCPE Bull.* **1990**, *10*, 52.
(23) Stewart, J. J. P. QCPE, program 455.
(24) Davidson, N. *Statistical Mechanics*; McGraw-Hill: New York, 1962.
(25) Boatz, J. A.; Gordon, M. S. *J. Phys. Chem.* **1989**, *93*, 1819. Pulay, P.; Torok, F. *Acta Chim. Acad. Sci. Hung.* **1966**, *47*, 276.
(26) Carsky, P.; Hess, B. A., Jr.; Schaad, L. J. *J. Comput. Chem.* **1984**, *5*, 280.

Table III. Minima (ϕ; ω; τ) Located on the Conformational PES of Glycine

conformer	idealized conformation	6-31G*	STO-2G	AM1	PM3
GLY9	(0; 0; −120)	(0.2; 21.8; −106.5)	(−0.6; 22.3; −113.1)		
GLY10	(0; 60; −120)				(−1.5; 54.0; −116.7)
GLY11	(0; 120; 0)		(0.3; 148.6; −4.0)		
GLY12	(0; 120; 120)	(−2.1; 137.8; 124.7)	(−1.7; 125.7; 117.8)	(−2.7; 133.8; 110.5)	(−2.6; 134.2; 108.9)
GLY13	(180; 0; 120)	(−177.5; 21.3; 99.1)	(−178.7; 21.2; 102.6)		
GLY14	(180; 120; −120)		(178.8; 115.0; −129.6)	(−178.4; 141.5; −138.1)	(−177.0; 136.7; −131.3)
GLY15	(180; 120; 0)		(172.5; 110.1; −3.5)	(175.5; 113.3; −17.7)	
GLY16	(180; 180; −120)	(−178.6; 163.8; −150.1)	(−175.9; 160.2; −143.4)		

analysis as large deviations (from 6-31G* values) in the CC–O and NCC angles. These angles are overestimated by 7.4° and 1.7°, respectively, by AM1, whereas the usual overestimation is lower (see Table II). Thus, the elongated OH···N distance is due to a larger than average distortion of the AM1 structure. This is probably due to a repulsion between the OH and N groups, whereas 6-31G* predicts an attraction, presumably due to hydrogen bonding. Performing RHF/6-31G* single-point energies on the AM1 structures leads to a 2 kcal/mol lowering in the relative energy for GLY3. The narrow energy spread for GLY6, GLY8, and GLY4 is preserved. The relative energy of GLY3 (7.5 kcal/mol) is also overestimated by RHF/6-31G*//PM3, as is the relative energy of GLY8 (13.1 kcal/mol). The former indicates that the PM3 structure deviates significantly from the one calculated with RHF/6-31G*. Indeed, the CC–O angle is overestimated by 8.3°, and the OH···N distance is 2.31 Å. Thus, it appears that while the hydrogen-bonding parametrization of PM3 results in a relatively good energy (4.2 kcal/mol) for GLY3, it does not result in a good structure, at least compared to the RHF/6-31G* result.

Table II lists the average and standard deviations (relative to the 6-31G* values) for 15 internal parameters of the eight C_s conformations of glycine. Both semiempirical methods perform well for bond lengths, the largest deviation being −0.05 Å for r(C=O), calculated with AM1. The STO-2G basis set does consistently worse for bond lengths, with the exception of r(CH). Bond angles are well predicted on average by all methods, although AM1 does the best for most angles. All methods do fairly well for dihedral angles, with the exception of D(CCNH), for which STO-2G predicts an average deviation of 0.0 ± 6.7°. The remaining deviations are all at or below 1.0°.

The hessian was calculated for all eight conformations, and the eigenvalues were extracted upon diagonalization. The 6-31G* basis set predicts four minima (GLY1, GLY2, GLY4, and GLY5), three transition states (GLY3, GLY6, and GLY7), and one conformer with two imaginary frequencies (GLY8). The four minima are the four conformers for which D(CCNH) ≈ ±60°. The semiempirical Hamiltonians predict (Table I) GLY1, GLY2, and GLY4 to be minima, but both predict one small (<50i cm^{-1}) imaginary frequency for GLY5. STO-2G predicts small imaginary frequencies for GLY2 (35.2i cm^{-1}) and GLY5 (36.9i cm^{-1}). All methods predict one imaginary frequency for GLY3 and GLY7, except PM3 predicts an extra imaginary frequency (16.4i cm^{-1}) for GLY7. Both semiempirical methods predict two imaginary frequencies for GLY6, whereas STO-2G only predicts one. Finally all methods predict two imaginary frequencies for GLY8. Thus, all methods deviate from the 6-31G* results by predicting spurious small imaginary frequencies for some conformers. This is most likely due to the use of a minimal basis set. Attempts to remove these small frequencies by decreasing the gradient-convergence criteria for those structures led to frequency changes of less than 2 cm^{-1}.

To provide additional insight, the mass-weighted dot products of the eigenvectors associated with the GLY3 and GLY7 imaginary frequencies from 6-31G* and STO-2G or AM1 were calculated. These DMC indices for GLY3 are 0.969 and 0.996 for STO-2G and AM1, respectively, and 0.990 and 0.995 for GLY7. This is especially encouraging, since it suggests that one can trace the MEP to products and reactants with AM1 and be fairly confident that the end points are the same for 6-31G*. This results in a significant saving of computer time.

Thus, the AM1 gradient was followed downhill for GLY3 and GLY7. The GLY3 conformer was found to be the transition state connecting a C_1 minimum with its mirror image, and will be discussed in detail later. The GLY7 conformer was found to be the transition state for the barrier for the C–N rotation of GLY4, with barrier heights of 6.8 and 6.6 kcal/mol predicted by MP2/6-31G* and RHF/6-31G*, respectively. Unfortunately, both semiempirical methods predict two imaginary frequencies for GLY6, so the same procedure cannot be used in this case. However, by examining the normal mode associated with the imaginary frequency, one can make a reasonable guess at the nature of the transition state. From this, it appears that GLY6 is the transition state for the complete C–N rotation of GLY1, resulting in MP2/6-31G* and RHF/6-31G* barrier heights of 5.8 and 5.6 kcal/mol, respectively.

In summary, within C_s symmetry, electron correlation has only a minimal effect on the relative energies. Relative energies, calculated with MP2/6-31G*//RHF/6-31G*, are duplicated well by RHF/6-31G*//RHF/6-31G* and RHF/6-31G*//RHF/STO-2G, and less well by the other methods. Geometries are generally well predicted by all methods, although the semiempirical methods do not handle intramolecular hydrogen bonding well. The RHF/6-31G* basis set predicts four minima, three transition states, and one stationary point with two imaginary frequencies (GLY8). The latter is predicted by all methods. STO-2G finds only two minima, whereas AM1 and PM3 both predict three. The PM3 method predicts a second conformer with two imaginary frequencies (GLY7). The nature of all three 6-31G* transition states is established.

B. C_1 Conformers. 1. Minima. As mentioned in the Introduction, nonionized glycine has three internal rotation degrees of freedom. These can be defined as three torsional angles, ϕ, ω, and τ, for the rotation about the C–O, C–C, and C–N bonds, respectively. The GLY1 conformer, for example, is arbitrarily defined as the conformation for which (ϕ; ω; τ) = (0; 0; 0). Thus, one can construct 36 conformations (ϕ = 0, 180; ω = −120, −60, 0, 60, 120, 180; τ = −120, 0, 120) for which the steric repulsion of all atoms appears to be minimal and that therefore represent possible minima on the PES. Sixteen of these conformations have equivalent energies due to symmetry: $E(\phi; \omega; \tau) = E(\phi; -\omega; -\tau)$, where ϕ = 0, 180; ω = 0, 60, 120, 180; τ = 0, 120; and $E(\phi; \omega; \tau)$ = the energy of conformation (ϕ; ω; τ). Four of the remaining 20 energy unique conformations have C_s symmetry (0, 180; 0, 180; 0) and were discussed in the previous section. This leaves 16 possible C_1 minima on the conformational PES (0, 180; 0, 60, 120, 180; 0, 120), all of which were used as initial guesses for full optimizations using AM1, PM3, and STO-2G. Any stationary points located with one or more of these methods were then used as initial guesses for RHF/6-31G* optimizations.

The conformations of the resulting C_1 minima found on the PES are listed in Table III and depicted in Figure 1 together with the C_s minima. It is apparent that the nature of the surface is very dependent on the method used. In fact, only one C_1 minimum, GLY12 (0; 120; 120), is predicted by all methods. With use of the 6-31G* basis set, three additional minima are located: GLY9 (0; 0; −120), GLY13 (180; 0; 120), and GLY16 (180; 180; 120). All four minima are also predicted by STO-2G, which predicts three additional minima: GLY11 (0; 120; 0), GLY14 (180; 120; −120), and GLY15 (180; 120; 0). In addition to GLY12, AM1 predicts two other minima: GLY14 and GLY15. With use of PM3, a new minimum is found, GLY10 (0; 60; −120), in addition

Table IV. Energies, Relative to GLY1 (kcal/mol), of the C_1 Conformational Minima

basis set	GLY9	GLY10	GLY11	GLY12	GLY13	GLY14	GLY15	GLY16
MP2/6-31G*//RHF/6-31G*	2.2			3.2	8.9			1.5
RHF/6-31G*//RHF/6-31G*	2.2			3.1	9.3			2.9
RHF/STO-2G//RHF/STO-2G	1.4		0.6	1.3	6.0	7.3	6.4	1.2
PM3//PM3		2.1		2.5		3.5		
AM1//AM1				3.5		7.6	7.9	

Table V. Energy (kcal/mol) of the Highest Energy Conformer on a LLMP, Connecting the Conformation Heading the Column with the One Heading the Row, Relative to the Conformation Heading the Column

conformation	GLY1	GLY2	GLY4	GLY5	GLY9	GLY9M	GLY12	GLY12M	GLY13	GLY13M	GLY16	GLY16M
GLY1		2.0	7.0	9.6	0.6	0.6	5.9	5.9	6.7	6.7	20.1	20.1
GLY2	3.9		11.6	8.3	6.5	6.5	2.4	2.4	13.7	13.7	19.8	19.8
GLY4	14.0	16.7		2.6	14.6	14.6	21.2	21.2	0.4	0.4	11.5	11.5
GLY5	18.9	15.7	4.9		20.6	20.6	18.7	18.7	5.6	5.6	17.0	17.0
GLY9	2.7	6.7	9.7	13.4		4.3	3.2	3.8	6.3	11.2	17.6	14.6
GLY12	9.0	3.5	17.2	12.5	4.2	4.8		4.8	10.5	12.6	13.6	14.0
GLY13	16.0	21.1	2.7	5.6	13.5	18.4	16.8	18.8		5.2	5.0	4.6
GLY16	23.0	20.8	7.4	10.7	18.5	15.4	13.4	13.8	2.4	2.0		0.4

to GLY12 and GLY14. One would thus conclude that STO-2G is the best starting level for the investigation of this particular surface, since it is the only method that identifies all minima found by 6-31G*.

All four 6-31G* C_1 minima deviate significantly in the two torsional angles, ω and τ, relative to their idealized values. The largest deviation occurs for GLY16, for which τ deviates by 30° and ω by 16°. Such large deviations are also observed in the minima predicted by the other methods. This often makes it difficult to categorize the minima properly. For example, one might argue that the AM1 and PM3 structures labeled GLY14 really are halfway between GLY14 and GLY16. The deviations in ϕ are always less than 5°. Comparing torsional parameters for GLY12, one finds that most methods do relatively well compared to 6-31G*. The largest deviation is in τ, which is underestimated by 16° by PM3.

Table IV lists the energies, relative to GLY1, of the conformations listed in Table III. Three of the minima on the 6-31G* surface have low relative energies: GLY9 (2.1 kcal/mol), GLY12 (3.1 kcal/mol), and GLY16 (2.9 kcal/mol). The fourth conformer, GLY13, is much higher in energy, 9.3 kcal/mol above GLY1 (but <1 kcal/mol above the C_s minimum GLY5). Note that adding correlation reverses the relative energies of GLY9 and GLY16. All remaining methods, STO-2G, AM1, and PM3, predict low relative energies for GLY12, in agreement with 6-31G*. The STO-2G basis set predicts roughly the same order of stability for GLY9, GLY12, GLY13, and GLY16 as MP2/6-31G*.

2. Transition States. Having apparently located all minima on the RHF/6-31G* conformational PES, an effort was made to locate conformational transition states connecting various minima. Linear least motion paths (LLMP's) were constructed for all possible combinations of minima, at the RHF/6-31G* level of theory. To be complete, one has to include the mirror conformers ($-\phi$; $-\omega$; $-\tau$), labeled GLYXM (X = 9, 12, 13, 16) in certain instances. The following types of LLMP's were considered:

$$\text{GLY}X \leftrightarrow \text{GLY}Z \qquad X, Z = 1, 2, 4, 5, 9, 12, 13, 16 \quad X < Z$$

$$\text{GLY}X \leftrightarrow \text{GLY}Z\text{M} \qquad X, Z = 9, 12, 13, 16 \quad X \le Z$$

This selection is exhaustive. The resulting LLMP barriers are listed in Table V. A 3-21G hessian[27] was computed at the geometry of the highest energy structure on each LLMP to determine the number of imaginary frequencies. High-energy conformers having one or two imaginary frequencies were then chosen as initial guesses for RHF/6-31G* optimizations to locate a proper saddle point, i.e., a geometry with one and only one imaginary frequency. Fifteen C_1 transition states have been identified in this manner, and the resulting barriers for the 15 conformational rearrangements are listed in Table VI. All other conformational changes were either judged unlikely to have proper transition states, on the basis of the fact that the geometry had three or more, rather large (~300i cm^{-1}), imaginary frequencies, or failed to converge to a proper transition state during optimization. In addition, GLY3 is included as the transition state for reaction 16.

Both barriers and imaginary frequencies span a rather wide range for conformational rearrangements. Barriers up to 15 kcal/mol (GLY2 → GLY5) and as low as 0.1 kcal/mol (GLY13 → GLY4) are predicted. The latter implies a very flat region of the surface and may not correspond to a real barrier to internal

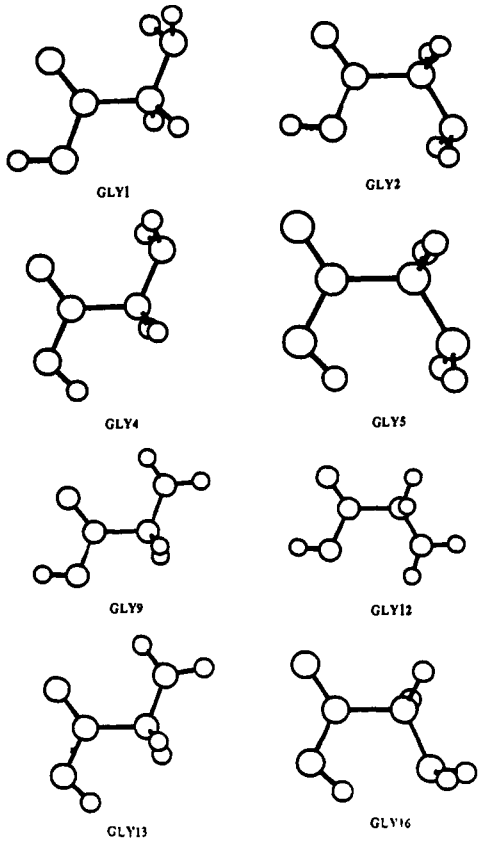

Figure 1. Optimized structures of the eight minima found on the conformational PES of gas-phase glycine.

(27) To economize computer time, the hessians were not calculated with the 6-31G* basis set. Instead, the 3-21G basis set was used after it had been judged to be sufficiently accurate, by a few comparative calculations with 6-31G*. The STO-3G basis set was considered as well but rejected since the imaginary frequencies were much too large in magnitude, compared to 6-31G* calculations.

Table VI. Barriers (kcal/mol) and Imaginary Frequencies (Unscaled; cm^{-1}) for Conformational Rearrangements[a]

conformational rearrangement	unoptimized			optimized				
	3-21G	barriers		6-31G*	RHF		MP2	
	freq	fwd	rev	freq	fwd	rev	fwd	rev
1. GLY1 ↔ GLY2	20li	3.9	2.0	58i	3.2	1.3	2.8	1.3
2. GLY1 ↔ GLY4	754i, 202i	14.0	7.0	556i	13.5	6.5	14.1	6.5
3. GLY1 ↔ GLY9	354i, 95i	2.7	0.6	211i	2.5	0.5	2.6	0.4
4. GLY2 ↔ GLY4	764i, 225i	16.7	11.6	529i	14.2	9.1	14.7	10.0
5. GLY2 ↔ GLY5	772i, 195i	15.7	8.3	549i	14.3	7.0	15.0	8.4
6. GLY2 ↔ GLY12	365i, 134i	3.5	2.4	287i	3.3	2.3	3.5	3.0
7. GLY4 ↔ GLY5	213i, 95i	4.9	2.6	37i	4.0	1.7	3.8	1.9
8. GLY4 ↔ GLY13	327i, 185i	2.7	0.4	182i	2.5	0.2	2.5	0.1
9. GLY4 ↔ GLY16	397i, 219i	7.4	11.5	84i	3.5	7.6	3.7	8.7
10. GLY5 ↔ GLY9	768i, 358i	13.4	20.6	529i	6.8	14.0	8.1	14.3
11. GLY5 ↔ GLY13	384i, 209i	5.6	5.6	318i	3.6	3.6	3.9	3.4
12. GLY9 ↔ GLY12	305i, 178i	4.2	3.2	31i	2.2	1.2	2.2	1.2
13. GLY9 ↔ GLY12M	214i, 165i	4.8	3.8	91i	4.1	3.1	3.7	2.7
14. GLY9 ↔ GLY16M	774i, 191i	15.5	14.6	587i	13.0	12.2	14.0	14.7
15. GLY13 ↔ GLY16M	224i, 22i	2.0	4.6	89i	1.1	7.5	1.2	8.6
16. GLY16 ↔ GLY16M	117i[b]	0.4	0.4	111i	0.3	0.3	0.2	0.2

[a] Barriers are calculated with RHF/6-31G* or MP2/6-31G*. fwd = forward; rev = reverse. [b] This frequency was calculated at the RHF/6-31G* level of theory.

Table VII. Previously Calculated Relative Energies (kcal/mol) for Various Glycine Conformers, Compared to Values Obtained in This Study[‡]

basis set	GLY1	GLY2	GLY3	GLY6	GLY8	GLY4	GLY5	GLY7
MP2/6-31G*//RHF/6-31G*[‡]	0.0	1.7	1.8	5.8	6.5	6.5	8.4	13.3
RHF/4-31G[1]	0.0	2.6	2.2	8.1	7.5			
RHF/4-21G//RHF/4-21G[6]	0.0	1.9	2.2					
RHF/STO-3G//RHF/STO-3G[11]	0.0	0.9	1.8	4.7	6.0	4.8	8.8	10.5
RHF/STO-2G//RHF/STO-2G[‡]	0.0	0.6	2.0	4.8	5.8	4.1	7.7	9.8

rotation. The barriers listed in Table VI do not include zero-point energy (ZPE) corrections. They will be addressed in the section on temperature effects. The MP2 energy corrections have little effect ($\leq$1 kcal/mol) on the barriers, as was observed for the relative energetics of the glycine minima. The magnitude of the imaginary frequencies range from 31 to 587 cm^{-1}. The larger frequencies are all associated with the rotation of the OH group; in fact, the magnitude of the imaginary frequency seems related to the mobility of the OH group. For example, the imaginary frequency of reaction 12 corresponds largely (74%) to a change in ω, while the ϕ contribution is minuscule. On the other hand, reaction 14 corresponds almost entirely to ϕ rotation.

Most barriers predicted by the LLMPs are within 1–2 kcal/mol of the optimized barriers. Discrepancies are larger for higher barriers, and relative accuracies are therefore very good. Analogous considerations of the imaginary frequencies cannot be made since the vibrational analysis of the hessian is valid only at stationary points.

C. Comparisons to Previous Calculations. Most of the previous studies of the conformational PES of glycine have been largely concerned with a few or all of the eight C_s conformers. The relative energies of these, presented in previous studies plus a subset from this study for comparison, are presented in Table VII. It is apparent that using standard bond lengths and bond angles is inadequate for the prediction of relative stabilities,[1] possibly due the inadequate treatment of steric repulsions for certain conformers (GLY2 and GLY6), which leads to overestimation of energies. Thus, when the three lowest energy conformers were optimized by Schäfer et al.,[6] with a slightly smaller basis set, the relative stability was well reproduced relative to MP2/6-31G*. The RHF/STO-3G relative energies calculated by Lucas et al.[11] show the same trends found with RHF/STO-2G in this study; i.e., the relative energy of GLY4 is underestimated (by 1.7 kcal/mol), but other stabilities are well reproduced.

In addition to C_s stationary points, a few earlier studies included C_1 conformations. Vishveshwara and Pople,[1] for example, predicted a shallow minimum at around (0; 120; 120) with a relative energy of 4 kcal/mol. This compares quite well to GLY12 of this study, with a MP2/6-31G* relative energy prediction of 3.1 kcal/mol. The GLY9 conformer was not found, although a rather flat region is indicated by the conformational potential energy map (Figure 1[1]) of that study in the (0; 60; −120) region. Only the part of the PES for which $\phi = 0°$ was considered in their study, so the remaining two minima predicted by RHF/6-31G* were not observed. In addition, Vishveshwara and Pople[1] suggested a transition state (Figure 4b[1]) for the GLY1 ↔ GLY2 rearrangement around (0; 90; 0), which agrees quite well with the transition state found for that rearrangement in this study: GLYTS1 (−0.2; 85.8; 1.8).

The results obtained by Palla et al.[7] for the RHF/STO-3G conformational PES of nonionized glycines exemplify the difficulties one encounters when using minimal basis sets and conformational PE maps for this problem. Apparently, the maps (Figures 6 and 7 in ref 7) are not detailed enough to indicate all possible minima. By inspection, one does not find GLY9, GLY11, GLY13, or GLY16. This is especially unfortunate since most of these were predicted by RHF/6-31G* in this study. Thus, this surface misses many important points found on the RHF/6-31G* surface.

Finally, a comment is in order regarding the structure observed independently by Brown et al.[2] and by Suenram and Lovas[3] in the microwave spectrum of glycine. Sellers and Schäfer[6] postulated that this structure is GLY3, and Ramek's[14] work at the 4-31G level of theory seems to support this. However, the current work has shown GLY3 to be a transition state connecting GLY16 with its mirror image, with a tiny (0.2 kcal/mol) barrier. When ZPE is included, this barrier disappears (and an equally tiny Gibbs free energy barrier reappears at higher temperatures). This reflects the very flat potential energy region in this part of the surface and illustrates the essentially free internal rotation connecting GLY16 with GLY16M. This explains why GLY3 is observed in the microwave spectrum, since GLY3 represents the geometric average between the two conformations. This part of the surface seems quite basis set dependent, so GLY3 was also optimized at the RHF/6-311G** level of theory, resulting in only a 3-cm^{-1} decrease in the imaginary frequency. Thus, it seems that the nature of the GLY3 conformer has been correctly established by both experiment and theory.

D. Temperature Effects. This section concerns itself with the effect of temperature upon the conformational PES. Toward this end, Gibbs free energies are computed at various temperatures and used to evaluate equilibrium distributions and rate constants

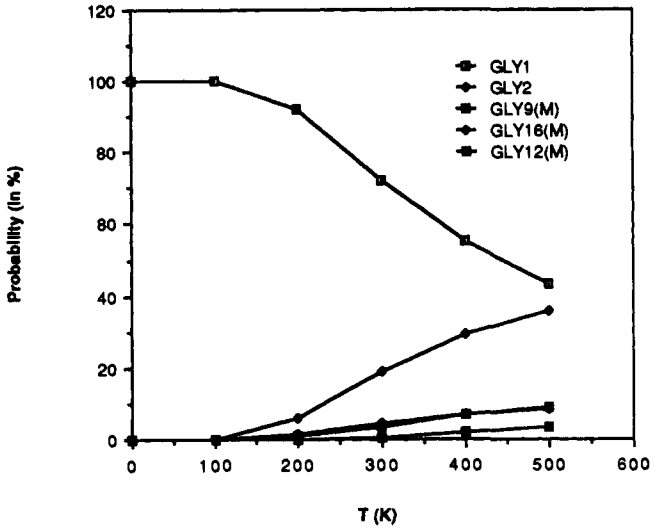

Figure 2. Equilibrium composition of glycine in the temperature range 0–500 K, as a plot of the percent probability vs T. Notice that GLY16M should be considered in conjunction with GLY3.

for conformational interconversions. The use of the harmonic oscillator–rigid rotor approximation is implicit in these calculations, and caution should be exercised when properties calculated at high temperature and/or flat regions of the PES are analyzed. The numbers presented are semiquantitative at best, but trends presented in this section are most likely correct nevertheless.

1. Equilibrium Distribution. The preceding discussion has focused on electronic energy differences. Relative energies that include ZPE corrections correspond to enthalpy differences at 0 K (ΔH_0). As the temperature is increased, more vibrational levels will be occupied (enthalpy increase) and entropy differences can play a role. Thus, the relative stabilities at $T > 0$ K are best represented by relative Gibbs free energies ΔG_T (note that $\Delta H_0 \equiv \Delta G_0$).

To investigate the effect of temperature on the relative stabilities of the glycine minima, ΔG_T was computed for T = 0–500 K, in steps of 100 K, by using MP2/6-31G* energies as the electronic energy contribution. The relative free energies can be used to predict the Boltzmann equilibrium distribution of glycine among the available minima:

$$p_T(i) = \frac{e^{-\Delta G_T(i)/RT}}{\sum_i e^{-\Delta G_T(i)/RT}}$$

In this expression, $\Delta G_T(i)$ is the Gibbs free energy of conformation i at temperature T, relative to the global minimum (ΔG_T(GLY1) ≡ 0), and R is the ideal gas constant.

Figure 2 shows how the equilibrium distribution of a glycine gas varies with T. One can see that most glycine molecules are in the global minimum conformation (GLY1) at T = 0–100 K, but as the temperature is increased further, more and more molecules assume the GLY2 geometry; i.e., the relative Gibbs free energy of GLY2 decreases. The dramatic decrease of ΔG_T(GLY2) is due to a rather large entropy term. In the range 100–500 K, the GLY2 conformation has an entropy that is 3 cal/mol·K larger than the average entropy of all minima (σ_{std} = 1 cal/mol·K). This may be traced to a large vibrational entropy term arising from a very low (16 cm^{-1}) frequency; the lowest frequencies in the other minima range from 70 to 110 cm^{-1}. This 16-cm^{-1} frequency contributes 91–37% to the vibrational entropy in that temperature range and is a prime contributor at all T. The 16-cm^{-1} frequency corresponds to an a″ mode and is displayed in Figure 3. This motion may be strongly coupled with the reaction coordinate of GLY2 → GLY1, since the mode corresponds almost exclusively to ω rotation. Given the low barrier of this reaction (ΔH_0 = 0.9 kcal/mol), this surface is likely to be very flat, giving rise to the very low frequency. At 300 K, the equilibrium composition is comprised of 72% GLY1 and 19% GLY2, while other conformations make minor contributions. At all temperatures, >99% of the composition is accounted for by the five conformations included in Figure 1.

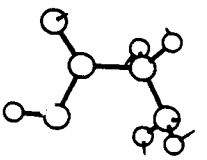

Figure 3. a″ normal mode associated with the lowest vibrational frequency of the GLY2 conformation.

2. Kinetics. The relative probability for finding glycine in a particular minimum does not reveal the ease with which that minimum is reached. The latter is primarily a function of the barrier that has to be surmounted to reach the minimum and the associated kinetics. Table VI appears to list all barriers on the conformational PES associated with a proper transition state and to which kinetic considerations can be applied. Given the barriers and the equilibrium partition functions for reactants and transition states (Q_R and Q^*, respectively), one can calculate the classical rate constants using conventional transition state theory (TST)[28]:

$$k^{TST} = \frac{k_B T}{h}\frac{Q^*}{Q_R} e^{-\Delta G_T/RT}$$

Here, k_B and h are the Boltzmann and Planck constants, respectively. The classical rate constant k^{TST} does by definition not include quantal effects such as tunneling, and an ad hoc correction must be included. This usually is done by introducing a transmission coefficient (κ) calculated by some method. In this study, the augmented Wigner correction[29]

$$\kappa = 1 + \frac{1}{24}\left|\frac{h\nu^*}{k_B T}\right|^2\left(1 + \frac{RT}{\Delta G_T}\right)$$

has been used. In this expression, ν^* is the imaginary frequency of the transition state.[30] The final rate constant is thus given by

$$k^{TST/w} = \kappa k^{TST}$$

($k^{TST/w}$ is hereafter referred to as k).

Forward and reverse rate constants (k_f and k_r, respectively) were calculated for the reactions listed in Table VI at T = 100–500 K in increments of 100 K. Reactions 8 and 16 were excluded, since these barriers disappared when ZPE was included. The resulting rate and equilibrium constants ($K_{eq} = k_f/k_r$) are listed in Table VII.

One point of interest is the ease of conversion of glycine from the global minimum to the other four conformers in Figure 2 as a function of temperature. For example, while the *equilibrium* composition of glycine at 300 K (based on the relative free energies of all eight minima) has about 15% more GLY2 than GLY9, the rate constants indicate that GLY1 → GLY9 is faster ($k = 2.8 \times 10^{10}$ s^{-1}) than GLY1 → GLY2 ($k = 5.8 \times 10^9$ s^{-1}) at the same temperature. This difference is even more pronounced at lower temperatures.

An interesting question concerns the possibility of different paths connecting the same two minima. One example is the path to GLY12 from GLY1. The GLY1 → GLY12 LLMP predicts a 9 kcal/mol barrier, but does not result in a proper transition state. The two most direct paths that emerge from this study are GLY1 → GLY2 → GLY12 and GLY1 → GLY9 → GLY12, paths 1 and 2, respectively. At 300 K, the rate-determining step for both

(28) A summary of transition state theory is given in Steinfield, J. I.; Francisco, J. S.; Hase, W. L. *Chemical Kinetics and Dynamics*; Prentice-Hall: Englewood Cliffs, NJ, 1989; Chapter 10.

(29) Formula taken from ref 29, p 320. Note typo.

(30) Although a rigorous evaluation of the tunneling probability requires an analysis of the reaction path [(a) Skodje, R. T.; Truhlar, D. G. *J. Phys. Chem.* **1981**, *85*, 624. (b) Truhlar, D. G.; Garret, B. C. *J. Chim. Phys. Phys.-Chim. Biol.* **1987**], *84*, 365. The Wigner correction provides qualitative trends in rate constants.

Table VIII. Forward and Reverse Rate Constants (s^{-1}) and Equilibrium Constants as a Function of Temperature (T, K)

	T				
	100	200	300	400	500
		Forward Rate Constants			
1. GLY1 ↔ GLY2	1.5E+06	8.7E+08	5.8E+09	1.3E+10	2.1E+10
2. GLY1 ↔ GLY4	2.7E-16	3.3E-02	1.8E+03	4.3E+05	1.2E+07
3. GLY1 ↔ GLY9	1.4E+07	4.6E+09	2.8E+10	6.6E+10	1.1E+11
4. GLY2 ↔ GLY4	8.0E-19	4.6E-04	4.3E+01	1.3E+04	4.2E+05
5. GLY2 ↔ GLY5	3.1E-19	2.7E-04	2.8E+01	9.5E+03	3.1E+05
6. GLY2 ↔ GLY12	3.2E+04	8.0E+07	1.0E+09	3.6E+09	7.1E+09
7. GLY4 ↔ GLY5	4.8E+03	5.8E+07	1.1E+09	4.3E+09	9.3E+09
9. GLY4 ↔ GLY16	5.1E+03	5.4E+07	9.7E+08	3.7E+09	7.8E+09
10. GLY5 ↔ GLY9	5.6E-04	6.4E+04	3.3E+07	7.3E+08	4.5E+09
11. GLY5 ↔ GLY13	8.7E+03	1.4E+08	3.4E+09	1.6E+10	3.6E+10
12. GLY9 ↔ GLY12	1.1E+07	2.8E+09	1.5E+10	3.2E+10	4.7E+10
13. GLY9 ↔ GLY12M	1.1E+04	9.9E+07	1.8E+09	6.8E+09	1.5E+10
14. GLY9 ↔ GLY16M	2.1E-16	3.5E-02	2.1+03	5.3E+05	1.5E+07
15. GLY13 ↔ GLY16M	8.0E+08	2.0E+10	4.7E+10	6.5E+10	7.4E+10
		Reverse Rate Constants			
1. GLY1 ↔ GLY2	8.3E+08	4.1E+09	5.9E+09	6.3E+09	6.2E+09
2. GLY1 ↔ GLY4	5.4E+00	4.9E+06	5.1E+08	5.1E+09	2.1E+10
3. GLY1 ↔ GLY9	1.0E+12	1.3E+12	1.3E+12	1.2E+12	1.1E+12
4. GLY2 ↔ GLY4	1.0E-07	8.6E+02	1.8E+06	8.2E+07	8.1E+08
5. GLY2 ↔ GLY5	2.1E-04	3.6E+04	2.1E+07	5.1E+08	3.3E+09
6. GLY2 ↔ GLY12	6.1E+06	5.2E+09	4.7E+10	1.3E+11	2.4E+11
7. GLY4 ↔ GLY5	2.5E+07	4.1E+09	1.9E+10	3.7E+10	5.1E+10
9. GLY4 ↔ GLY16	9.7E-07	1.0E+03	1.0E+06	3.1E+07	2.3E+08
10. GLY5 ↔ GLY9	8.1E-17	2.5E-02	1.8E+03	5.0E+05	1.5E+07
11. GLY5 ↔ GLY13	1.3E+04	1.7E+08	3.6E+09	1.5E+10	3.5E+10
12. GLY9 ↔ GLY12	2.2E+09	3.6E+10	7.6E+10	9.9E+10	1.1E+11
13. GLY9 ↔ GLY12M	2.0E+06	1.2E+09	8.6E+09	2.1E+10	3.5E+10
14. GLY9 ↔ GLY16M	5.4E-17	2.4E-02	2.3E+03	7.4E+05	2.5E+07
15. GLY13 ↔ GLY16M	1.6E-06	1.3E+03	1.2E+06	3.4E+07	2.5E+08
		Equilibrium Constants			
1. GLY1 ↔ GLY2	1.9E-03	2.1E-01	9.8E-01	2.1E+00	3.4E+00
2. GLY1 ↔ GLY4	5.1E-17	6.7E-09	3.6E-06	8.3E-05	5.7E-04
3. GLY1 ↔ GLY9	1.7E-05	3.9E-03	2.3E-02	5.7E-02	9.8E-02
4. GLY2 ↔ GLY4	7.7E-12	5.3E-07	2.4E-05	1.6E-04	5.2E-04
5. GLY2 ↔ GLY5	1.5E-15	7.5E-09	1.4E-06	1.9E-05	9.5E-05
6. GLY2 ↔ GLY12	5.3E-03	1.5E-02	2.3E-02	2.7E-02	3.0E-02
7. GLY4 ↔ GLY5	1.9E-04	1.4E-02	5.7E-02	1.2E-01	1.8E-01
9. GLY4 ↔ GLY16	5.2E+09	5.2E+04	9.4E+02	1.2E+02	3.3E+01
10. GLY5 ↔ GLY9	6.9E+12	2.6E+06	1.8E+04	1.4E+03	3.1E+02
11. GLY5 ↔ GLY13	5.3E-02	2.4E-01	4.2E-01	5.4E-01	6.2E-01
12. GLY9 ↔ GLY12	5.0E-03	7.8E-02	2.0E-01	3.2E-01	4.3E-01
13. GLY9 ↔ GLY12M	5.6E-03	8.4E-02	2.0E-01	3.2E-01	4.1E-01
14. GLY9 ↔ GLY16M	4.0E+00	1.5E+00	9.3E-01	7.1E-01	5.9E-01
15. GLY13 ↔ GLY16M	5.1E+14	1.5E+07	3.9E+04	1.9E+03	2.9E+02

paths is the second step, with respective rate constants of 1.0×10^9 vs 1.5×10^{10} s^{-1}. Path 2 is therefore favored over path 1. This is consistent with the lower net barrier for path 2. As expected, the difference is more pronounced as the temperature is decreased.

Equilibrium constants provide valuable information in addition to relative energies. When derived from transition-state theory, K_{eq} is not only a function of the exponential term $e^{-(\Delta G_{T,f}-\Delta G_{T,r})/RT}$, but also of $Q_{R,r}/Q_{R,f}$ (tunneling does not contribute to K_{eq}). The latter ratio becomes more important as the barriers approach the same magnitude. Some interesting temperature trends occur. Two examples of equilibrium reversal with increasing temperature are found on the conformational PES: GLY1 ↔ GLY2 and GLY9 ↔ GLY16M. The former equilibrium favors GLY1 at low temperatures ($K_{eq,T=100} = 0.002$) but is reversed, somewhat above room temperature, and at 500 K $K_{eq} = 3.4$. However, it is apparent (Figure 2) that although GLY2 approaches GLY1 in stability, GLY1 remains the global minimum at 500 K. So, the reversal cannot be caused entirely by the exponential term. Rather, as the difference in forward and reverse barrier heights approaches zero, Q_{GLY2}/Q_{GLY1} (which increases from 3.6 to 4.4 over the temperature range) becomes the predominant term, shifting the equilibrium in favor of GLY2. The equilibrium GLY9 ↔ GLY16M shifts in favor of GLY16M between 200 and 300 K due to the fact that the relative stabilities of GLY9 and GLY16M are reversed in that temperature range (and thus the relative probabilities; see Figure 1). Of course the barriers are reversed, which causes the shift in equilibrium.

Conclusions

The RHF/6-31G* conformational potential energy surface (PES) of nonionized glycine contains eight C_s stationary points (four minima, three transition states, and one structure with two imaginary frequencies), at least four additional energy unique (C_1) minima (Figure 1), and sixteen conformational transition states connecting various minima. The nature of the surface is basis set dependent and is not well reproduced by STO-2G, AM1, or PM3, since the former predicts too many, and the two latter, too few, minima relative to 6-31G*. Correlation appears to have little effect on relative energies.

The Boltzmann equilibrium distribution of glycine (Figure 2), calculated by using relative Gibbs free energies, indicates that the stabilities of the global minimum (GLY1) and the second lowest minimum (GLY2) approach one another with increasing temperature. At 300 K, the equilibrium distribution consists of 72% GLY1 and 19% GLY2. The explanation lies in the large vibrational entropy of GLY2 caused by a very low (16 cm^{-1}) a″ vibrational mode (Figure 3).

The kinetics of conformational interconversion is studied by using conventional transition-state theory with a simple Wigner tunneling correction. The interconversion of GLY1 to GLY12

occurs via GLY2 (i.e., GLY1 → GLY2 → GLY12) rather than GLY9, on the basis of relative rate constants presented in Table VIII. Equilibrium reversals, shown by calculating equilibrium constants (Table VIII), with increasing temperatures are observed for two different equilibria: GLY1 ↔ GLY2 and GLY9 ↔ GLY16M. The former is explained by the large equilibrium partition function of GLY2 relative to GLY1 (caused, again, by the large vibrational entropy of GLY2), which dominates the equilibrium constants as the difference in relative energies approaches zero. The latter is due to a reversal of stability of GLY9 and GLY16M as the temperature is increased (Figure 1).

Two main points emerge from the comparison of this with other studies. One is that conformational potential energy maps[1,7] have to be rather refined to locate all minima on the glycine PES. The second is that one conformation (GLY3, Scheme I) is a transition state on the electronic PES, but that the electronic barrier is so small that the vibrational energies of the normal modes are sufficient to overcome this barrier. Thus, this study suggests that GLY3 is the conformational average of the free internal interconversion between GLY16 and its mirror image, and hence observed in microwave spectra.[2,3]

Acknowledgment. This work was supported in part by a grant from the Petroleum Research Fund, administered by the American Chemical Society. Computer time was made available by the North Dakota State University Computer Center on its IBM 3090/200E, obtained via a joint study agreement with IBM. Additional calculations were carried out on a DECstation 3100 and a VAXstation 3200, both funded by a grant from the National Science Foundation (CHE86-40771). We would like to thank Nikita Matsunaga for drawing our attention to Dr. Ramek's paper. Helpful discussions with Dr. Michael Ramek, Dr. Walter Stevens, and Dr. Donald Truhlar are gratefully acknowledged.

Registry No. Gly, 56-40-6.

Supplementary Material Available: Tables listing bond lengths, bond angles, and dihedral angles of the eight C_s conformers of glycine, the four C_1 minima of glycine, and GLYTS1-15 (4 pages). Ordering information is given on any current masthead page.

Structures and Bonding of Group IV Sulfur and Oxygen Propellane Derivatives

Kiet A. Nguyen, Marshall T. Carroll,† and Mark S. Gordon*

Contribution from the Department of Chemistry, North Dakota State University, Fargo, North Dakota 58105-5516. *Received March 25, 1991*

Abstract: The RHF, ROHF, and GVB structures and energetics of group IV 2,4,5-trioxa[1.1.1]metallapropellanes, 2,4,5-trithia[1.1.1]metallapropellanes, and their bicyclopentane analogues have been determined from ab initio molecular orbital theory by using both the 6-31G(d) basis set for all-electron calculations and the valence basis set with effective core potentials (ECP) developed by Stevens, Basch, and Krauss. Although they have extremely short bridgehead distances, these species possess fairly large natural orbital occupation numbers in the lowest unoccupied molecular orbitals, indicating significant diradical character. Structures and other properties determined by ECP calculations are in good agreement with the 6-31G(d) all-electron calculations.

I. Introduction

Considerable attention has been given to group IV propellanes (**1**) (M = C, Si, Ge, Sn) and their derivatives in an effort to understand the nature of the bridgehead bonds (M_b-M_b). Despite a highly strained "inverted" tetrahedral arrangement at the bridgehead atoms, the simplest propellane (M = C) was successfully synthesized by Wiberg and co-workers.[1] This reactive compound (reacting rapidly with various reagents at the bridgehead positions[2]), with an experimental M_b-M_b bridgehead distance (1.60 Å)[3] that is slightly longer than the peripheral M_b-M_p bond (1.52 Å) and much shorter than the bridgehead bond (1.84 Å)[4] in bicyclo[1.1.1]pentane (**2**), has been a subject of discussion among both experimentalists[2,3,5] and theoreticians.[1,6,7-12] The silicon,[6,13-15] germanium[15,16a] and tin[15] analogues have also been theoretically investigated. Experimentally, pentasila-[1.1.1]propellane is not known, although a derivative (1,3-bis(4-*tert*-butyl-2,6-diisopropylphenyl)-2,2,4-tetraisopropylbicyclo-[1.1.1]pentasilane) of bicyclo[1.1.1]pentasilane has been synthesized recently.[16b] For germanium, neither the bicyclo form (**2**) nor the propellane form (**1**) has been experimentally observed.

Recently, an investigation of the structure and bonding of pentastanna[1.1.1]propellane and the analogues in group IV has been carried out this laboratory with use of the 3-21G(d) basis set and two different sets of effective core potentials developed

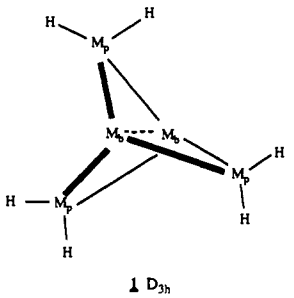

1 D_{3h}

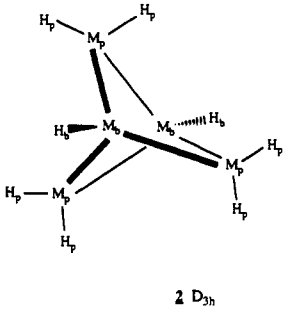

2 D_{3h}

by Stevens, Basch, and Krauss (SBK) and Wadt and Hay (WH). The singlet states were investigated at the restricted Hartree-Fock

† Natural Sciences and Engineering Council of Canada Postdoctoral Fellow.

(1) Wiberg, K. B.; Bader, R. F. W.; Lau, C. D. H. *J. Am. Chem. Soc.* **1987**, *109*, 985.
(2) Wiberg, K. B.; Waddell, S. T. *J. Am. Chem. Soc.* **1990**, *112*, 2194.
(3) (a) Wiberg, K. B.; Walker, F. H. *J. Am. Chem. Soc.* **1982**, *104*, 5239. (b) Wiberg, K. B.; Dailey, W. P.; Walker, F. H.; Waddell, S. T.; Crocker, L. S.; Newton, M. D. *J. Am. Chem. Soc.* **1985**, *107*, 7247.
(4) Wiberg, K. B.; Wendoloski, J. J. *J. Am. Chem. Soc.* **1982**, *104*, 5679.
(5) Wiberg, K. B. *Chem. Rev.* **1989**, *89*, 975.
(6) Schleyer, P. v. R.; Janoschek, R. *Angew. Chem., Int. Ed. Engl.* **1987**, *26*, 1267.
(7) Stohrer, W. D.; Hoffmann, R. *J. Am. Chem. Soc.* **1972**, *94*, 779.
(8) Newton, M. D.; Schulman, J. M. *J. Am. Chem. Soc.* **1972**, *94*, 773.
(9) Jackson, J. E.; Allen, L. C. *J. Am. Chem. Soc.* **1984**, *106*, 591.

0002-7863/91/1513-7924$02.50/0